Full Title

Essential Oil Bioactive Fibrous Membranes Prepared *Via* Coaxial Electrospinning

Name(s) of Author(s)

Zhi-Cheng Yao[a,b], Si-Cong Chen[c], Zeeshan Ahmad[d], Jie Huang[e], Ming-Wei Chang[a,b,*], Jing-Song Li[a]

Author Affiliation(s)

[a] Department of Biomedical Engineering, Key Laboratory of Ministry of Education, Zhejiang University, Hangzhou 310027, People's Republic of China.

[b] Zhejiang Provincial Key Laboratory of Cardio-Cerebral Vascular Detection Technology and Medicinal Effectiveness Appraisal, Zhejiang University, Hangzhou 310027, People's Republic of China.

[c] Clinical Research Center, The 2nd Affiliated Hospital, School of Medicine, Zhejiang University, Hangzhou 310009, People's Republic of China.

[d] Leicester School of Pharmacy, De Montfort, University, The Gateway, Leicester, LE1 9BH, UK.

[e] Department of Mechanical Engineering, University College London, London WC1E 7JE, UK.

Contact information for Corresponding Author

Ming-Wei Chang

College of Biomedical Engineering & Instrument Science, Zhe Da Road No.38, Zhou Yi Qing Building, Zhejiang University, Hangzhou, P.R. China, 310027

Tel.: +86 57187951517

Email address: mwchang@zju.edu.cn

Word count of text, for example

7,485 words

Short version of title

bioactive film for food preservation

Choice of journal/section

Food Engineering, Materials Science, and Nanotechnology

ABSTRACT:

A novel antimicrobial composite material was prepared by encapsulating orange essential oil (OEO) in zein prolamine (ZP) *via* the coaxial electrospinning (ES) technique. By manipulating process parameters, the morphological features of ZP/OEO fibers were modulated. Fine fibers with diameters ranging from 0.7 to 2.3 μm were obtained by regulating ZP solution concentration and process parameters during the ES process. Optimal loading capacity and encapsulation efficiency of OEO in fibrous ZP mats were determined to be 22.28% and 53.68%, respectively, and were achieved using a 35 w/v% ZP ES solution. The encapsulation of OEO was found to be reliant on ZP solution concentration (the enveloping medium). SEM analysis indicates the surface morphology of ZP/OEO electrospun fibers is dependent on ZP solution loading volume, with lower ZP concentrations yielding defective fibrous structures (e.g. beaded and spindled-string like morphologies). Furthermore, this loading volume also influences OEO loading capacity (LC), encapsulation efficiency (EE), mat water contact angle and oil retention. CCK-8 assay and cell morphology assessment (HEK293T cells) indicate no significant change with electrospun ZP and ZP/OEO fibrous membranes over an 8h period. Antimicrobial activity assessment using *Escherichia coli*, suggests composite non-wovens possess sterilization properties; elucidating potential application in active food packaging, food preservation and therefore sustainability.

Keywords:

zein prolamine; orange essential oil; food packaging; coaxial electrospinning.

Abbreviations:

ZP	Zein Prolamine
EO	Essential Oil
OEO	Orange Essential Oil
ES	Electrospinning
OM	Optical Microscopy
SEM	Scanning Electron Microscopy
LC	Loading Capacity
EE	Encapsulation Efficiency
WCA	Water Contact Angle
FTIR	Fourier Transform Infrared Spectroscopy

Practical Application:

Composite ZP/OEO fibrous membranes, fabricated using coaxial electrospinning (ES) technique, exhibit non-toxic in-vitro behavior and antimicrobial potential. This indicates their potential application for bioactive food packaging improving sustainability.

Introduction

It is envisaged up to 40% of the total food supply ends up as waste in developed countries, with food 'loss' the main cause. This is directly linked to preservation, retail sales and final consumption (Verghese and others 2015). Since food preservation is a crucial factor, advanced packaging materials may provide a valuable reduction in wastage (Chung and others 2003; Neo and others 2013). Food spoilage, caused by microorganisms, contributes towards waste and also poses an increased risk of foodborne illness (Gram and others 2002). Both of these outcomes have socioeconomic impacts, and it is therefore imperative to develop advanced packaging systems with antimicrobial properties capable of promoting quality and safety (Appendini and Hotchkiss 2002; Fernandez 2009; Gillgren and others 2009). Inclusion of actives into non-functional packaging materials (e.g. particles, films or wraps) have been shown to enhance shelf-life (Suppakul and others 2003). However, since there is a risk to oral exposure *via* ingestion or possible migration (Maisanaba and others 2014), it is paramount to assess toxic effects of emerging functionalized packaging materials.

Essential oils (EOs) are naturally occurring compounds displaying antimicrobial properties. EOs are categorized as GRAS (Generally Recognized as Safe) by the FDA (Wen and others 2016a) making them ideal for food preservation (Sugumar and others 2016). Several studies have shown chamomile blue, eucalyptus, lemongrass and lemon oils to exhibit antibacterial and antifungal properties (Liakos and others 2014; Friedman and others 2010; O'Bryan and others 2008). Citrus fruits possess high quantities of vitamins, minerals and flavonoids. The latter display antioxidant potential which is extremely valuable for anti-inflammatory and antimicrobial activity (Butz and others 2003). Moreover, amongst citrus oils, orange essential oil (OEO) exhibit interesting biological functions. OEO's have been part of human diet for hundreds of years, and

while they are currently used as additive ingredients, they have been shown to illicit preservative action; preventing growth of pathogens and spoiling microorganisms (Torresalvarez and others 2016). In particular, studies have shown the compounds citral and linalool to be key components for this action (Fisher and others 2007; Liu and others 2012). However, when exposed to open air or ultraviolet light, most EOs undergo oxidation (Alvarenga Botrel and others 2012). In addition, due to their water insolubility and highly volatile character, the application of EOs in food preservation has been limited (Wen and others 2016a; Moomand and Lim 2015a). For this reason, several studies have centered on EO stability and bioactive function while exploring their potential use in the food industry. For example, lemon essential oil has been encapsulated in non-ionic surfactant *via* a colloidal delivery system. Here the EO's properties were optimized by manipulating emulsion composition and altering storage conditions (Ziani and others 2012).

The electrospinning (ES) technique, a one-step preparation method, which has been used to engineer polymeric fibers on both nanometer and micrometer scales (Fabra and others 2016; Aceituno-Medina and others 2015). For this process, the surface tension of an electrically conducting formulation needs to be overcome by an applied electrical force; which ultimately enables ultra-fine fiber manufacturing. Resulting fibers are initially charged and under optimal conditions this permits further nano-scale modulation. Fiber charge and size are conventionally regulated through conventional process parameters (e.g. liquid flow rate and applied voltage) (Jaworek 2008). The coaxial ES process provides greater encapsulation opportunities such as micro/nano-layering, bioactive loading and controlled release. (McCann and others 2005).

Compared to other material engineering processes, ES enables fibrous film formation at the ambient environment and with an on-demand aspect. This makes the process friendlier towards volatile materials which may be susceptible to process damage. Fibers possess larger surface areas and also permit a breathable aspect due to inherent porosity control through over-layering. Furthermore, fiber accumulation over time enables film engineering with modulated fiber size which is known to impact active release properties and kinetics. In this regard, these variables allow thin films to be tailor-made for specific applications (Agarwal and others 2008; Quirós and others 2016). The encapsulation of OEO in to polymeric fibers using coaxial ES provides an opportunity to build on current single needle encapsulation work. This is beneficial, since OEO is volatile and complete (shell-like) encapsulation provides greater control on volatile material retention (e.g. EO's) (Chalco-Sandoval and others 2016). Another sister process, driven by formulation aspects, is emulsion ES. Here, additives within the ES medium (consisting of two phases), lead to complexity in process and have potential to impact food applications. Furthermore, the distribution of active (in emulsion form) is randomly distributed. With coaxial ES, well-defined polymer shell structures are achievable, with greater control on size distribution (narrow) making this more ideal than the related emulsion process (Hongxu Qi and others 2006; Jiang and others 2014). In addition, the ES encapsulation process facilitates EO stability and solubility by dispersing oils throughout the polymeric fibrous matrix. This improves EO spacing incorporating them closer to the molecular state rather than coarse oil droplets.

Zein prolamine (ZP) is a plant protein extract obtained from corn maize. Its intrinsic low hydrophilicity, exceptional membrane forming behavior, high thermal resistance and oxygen barrier properties make it ideal for numerous biological and biomedical

applications, including drug delivery and food technology. ZP has been used to encapsulate *via* both single needle and coaxial ES (Neo and others 2013; Yang and others 2013). Several studies have prepared ultra-thin ZP fibers to encapsulate bioactive components (Torres-Giner and others 2008; Jiang and others 2007). For example, ferulic acid (an antioxidant) has been blended with ZP to engineer composite systems with free-radical scavenging properties to improve drug delivery (Yang and others 2013).

In this study, composite ZP/OEO fibrous membranes were engineered *via* coaxial ES to demonstrate food preservation potential. OEO (the core medium) was encapsulated into the polymeric matrix of the enveloping medium (the shell material comprising ZP) functioning as a protective layer. The surface morphology, size distribution, and surface hydrophilicity of fabricated non-woven mats were modulated by varying engineering process parameters, such as ZP solution concentration, applied voltage, and media flow rate. The encapsulation potential of OEO, using solution parameters, was assessed by determining loading capacity (LC), encapsulation efficiency (EE) and oil retention. Mat biocompatibility and antimicrobial activity were assessed using HEK293T cell lines and *Escherichia coli* (*E. coli*), respectively. The results suggest the potential application of the composite electrospun membrane in active food packaging for food preservation and sustainability.

Materials and Methods

Materials

Zein prolamine (ZP, from maize corn) (Z 3625) was obtained from Sigma Aldrich (St.

Louis, Mo., USA). Ethanol, hexane and phosphate buffer saline (PBS, pH 7.4) were obtained from Sinopharm Chemical Reagent Co., Ltd (Shanghai, China). OEO extracted *via* steam-distillation was purchased from Jinyuan natural flavor Co., Ltd (Jiangxi, China). All chemicals were analytical grade and were used without further purification. A Millipore Milli-Q Reference ultra-pure water purifier (USA) was used to obtain deionized water (DI water) for experimentation.

Preparation of ZP solutions for electrospinning

Appropriate quantities of ZP powder were dissolved into aqueous ethanol (80 v/v%) to prepare several ZP solutions (25, 30 and 35 w/v%). A magnetic stirrer (VELP ARE heating magnetic stirrer, Italy) was used to ensure complete dissolution of ZP powder. The solutions were poured into a flask and then mechanically stirred at ~300 rpm at the ambient temperature (25°C) for 1 h.

Physical properties of solutions

Viscosities and electrical conductivities of ZP solutions with different concentrations were measured. Solution viscosity was measured using a viscometer (LVDV-II, Brookfield, USA). 2 mL of each solution sample was placed into pre-defined stainless steel wells of the viscometer and then the viscosity value was obtained at 25°C using a S21 spindle at 140 rpm. A YSI 3200 electrical conductivity meter (YSI, USA) was used to measure solution electrical conductivity at 25°C. All characterizations were carried out in triplicate and mean values were obtained.

Fabrication of electrospun composite ZP/OEO fiber

The coaxial ES apparatus (**Figure 1a**) includes a high power voltage supply, two

precision syringe pumps, a coaxial stainless steel needle and a collector connected to the ground electrode. The coaxial device consists of two concentrically aligned and enveloped needles. The diameter of the inner and outer needles were 0.2 and 0.4 mm, while the dimensions of the outer needle were 0.9 and 1.2 mm, respectively. A selected ZP solution was loaded into a 5 mL plastic syringe. A high-precision syringe pump (KD Scientific KDS100, USA) was used to perfuse the solution (in controlled fashion) from the syringe into the outer inlet of the coaxial stainless needle *via* silicon tubing. The inflow rate of ZP solution ranged from 1.5 to 3.0 mL/h. OEO was loaded into another syringe and perfused into the inner needle of the coaxial device at a flow rate of 1.5 mL/h. A high voltage power supply (Glassman high voltage Inc. series FC, USA) was used to generate an electric field between the coaxial needle and the ground electrode, and the voltage ranged from 18.0 to 19.5 kV. Aluminum foil, which was placed directly below the coaxial needle at a distance of 15 cm, was used as the collector and was connected to the grounded electrode. A high-speed camera (Baummer TXG02C, Germany) was used to observe the ES jetting modes. All experiments were performed at the ambient temperature (25°C).

Fiber morphology and size assessment

The morphology, diameter and size distribution of generated fibers were studied using optical (OM, Pheonix BMC503-ICCF, China) and field emission scanning electron microscopes (SEM, SU 8000 SEM, Hitachi, Japan). For SEM analysis, micrographs were obtained at an accelerating voltage of 20 kV. Samples were fixed on to metallic stubs by double-backed conductive tape. Prior to analysis, all samples were sputter-coated with a thin layer of gold using a vacuum sputter coater (Ion sputter MC 1000, Hitachi, Japan) for 60 s at a current intensity of 25 mA. Micrographs were

subsequently analyzed using ImageJ software (National Institute of Health, MD, USA) to measure fiber diameter at various process conditions. All statistical graphs were plotted using Origin software (OrginLab, USA).

Loading capacity and encapsulation efficiency of OEO

As a highly volatile medium, OEO at the fiber surface (un-encapsulated) is prone to evaporation (Li and others 2013). Thus, it is crucial to assess the encapsulation effect of OEO in ZP matrix. In this study, encapsulation properties of OEO were determined (loading capacity (LC) and encapsulation efficiency (EE)) following 2 h desiccation post engineering. According to previous studies (Neo and others 2013; Moomand and Lim 2014), these properties were determined by dissolving 100 mg of ZP/OEO composite fibers in 5 ml of 80 v/v% ethanol aqueous solution using a 15 mL centrifuge tube. After complete dissolution of composite fibers, OEO was extracted using 5 mL hexane for 15 min, and this procedure was carried out three times. OEO extracts were collected in 25 mL volumetric flasks, and the quantity of OEO was obtained using UV spectroscopy (UV-2600 spectrophotometer, Shimadzu, Japan). A wavelength of 202 nm was used to establish a standard calibration curve (Li and others 2013). The loading capacity (LC) of OEO in electrospun fibers was calculated by Equation 1:

$$\text{LC (\%)} = \frac{\text{Amount of oil content entrapped in the fibers}}{\text{Weight of the fibers}} \times 100\% \quad \text{(Eq.1)}$$

The encapsulation efficiency (EE) of OEO in the electrospun fibers was calculated using Equation 2:

$$\text{EE (\%)} = \frac{\text{Amount of oil content entrapped in the fibers}}{\text{Theoretical total amount of oil}} \times 100\% \quad \text{(Eq. 2)}$$

The theoretical quantity of OEO was calculated by obtaining the proportion of oil

weight to total weight of composite fibers, which was measured using solution density and the ratio of inner and outer layer solution flow rate. In this study, the theoretical amount of oil within 100 mg fibrous sample was 37 mg.

Water contact angle measurements

In general, water contact angle (WCA) measurements were used to represent the hydrophobic/hydrophilic nature of membranes. WCA's were measured using an optical contact angle meter (SL200KB, KINO Industry Co. Ltd., USA). The fibrous non-woven samples with thickness of ~0.1 mm were collected for 15 min and were subsequently layered onto an object slide using adhesive tape at the peripheral regions. WCA of pure OEO was measured by directly depositing the material onto a scribed object slide. The sample was mounted on to a three-axis horizontal tilt stage and the measurement was observed in the sessile drop mode at 25°C. A water droplet (~10 μL) was pipetted on to each membrane sample. The mean value of left and right WCAs on each sample was recorded, when the droplet status acclimatized (2 s after droplet release). The mean of three measurements was recorded.

Retention of OEO in fibrous membranes

OEO and electrospun ZP/OEO non-wovens (500 mg per sample, theoretically encapsulating 185 mg of OEO) were placed in 6 cm petri dishes. The samples were then placed into a forced air circulation oven (Heraeus T6, Thermo scientific, UK) at ambient temperature (25°C). The retention of OEO was defined as shown in Equation 3, which was calculated over a 24 h period. The analysis was carried out in triplicate.

$$\text{Retention (\%)} = \frac{\text{Total oil content}}{\text{Theoretical total amount of oil}} \times 100\% \quad \text{(Eq.3)}$$

Fourier transform infrared spectroscopy

Following OEO retention test (24 h), Fourier Transform Infrared (FTIR) spectroscopy (IR Affinity 1, Shimadzu, Japan) was used to assess material stability, identification and to determine any chemical interactions between encapsulated materials. Prior to FTIR scanning, pellet samples were prepared. Here the KBr pellet pressing method was deployed (Wang and others 2016). For this, 2 μL of OEO, 2 mg of pure ZP powder and 2 mg of ZP/OEO electrospun fibers were dispersed in 200 mg of KBr powder by grinding in a mortar, individually. The mixtures were then compressed into transparent pellets (pressure ~20 MPa). The spectrum (range ~ 4000 to 400 cm^{-1}) of each sample was acquired from 20 scans using a resolution of 4 cm^{-1}.

In-vitro biological evaluation

In food retail and manufacturing industries, deployed composite packaging materials are prone to consumer interaction, either through skin or oral contact. Therefore, it is necessary to assess potential risks of food packaging materials towards humans (Eleftheriadou and others 2016). In this study, HEK293T cell lines were used to assess cytotoxicity of ZP and ZP/OEO fibrous membranes. HEK293T cells were incubated and maintained in DMEM medium supplied with 10% FBS at 37 °C, in 5% CO_2. The culture medium was changed every 2 days. 100 μL HEK293T cell suspension was transferred to a 96-well plate at a density of 1.5×10^4 cells/well and incubated for 24 h. A CCK-8 assay was set to evaluate the proliferation of HEK293T cells at 4 and 8 h during cell culture. Electrospun fibrous non-wovens (collected for 1 h) were cut into discs (diameter = 6 mm). Fibrous discs were sterilized under UV light for 2 h and were then added to the cell culture plate. After incubation for 4 and 8 h, cell viability was measured by adding 20 μL of a CCK-8 solution to each well and incubating for a further

3 h. Absorbance was measured at a wavelength of 450 nm using a microplate reader (Multiskan GO, Thermo Fisher Scientific, USA). Cell viability in polystyrene well plate only was used as a control and the culture medium with CCK-8 solution was utilized as a blank. The relative cell viability (%) was calculated using Equation 4:

$$\text{Cell viability (\%)} = \frac{\text{Ab.(sample)-Ab.(blank)}}{\text{Ab.(control)-Ab.(blank)}} \times 100\% \quad \text{(Eq.4)}$$

Where Ab. means the absorbance.

In addition, optical microscopy (CKX41, Olympus, Japan) was utilized to observe cell morphology and to further confirm cell biocompatibility.

Antimicrobial activity test

Antimicrobial activity of electrospun membranes against *E. coli* was evaluated using an agar diffusion assay. Lysogeny-broth was sterilized in a High-pressure Steam Sterilization Pot (YXQ-LS-SⅡ, Shanghai Boxun Industry & Commerce Co., Ltd., Shanghai, China) at 120°C after which 10 mL was poured into several 10 cm petri dishes. 200 μL of bacterial suspension was spread on to agar plates once the nutrient medium had coagulated. Then, composite and pure electrospun ZP membranes (collected for 1 h and cut into 15 mm discs) were placed on to inoculated plates. The plates were incubated at 37°C for 24 h. Antimicrobial activity was evaluated by measuring disc inhibition zone as previously reported (Wen and others 2016a).

Statistical analysis

All experiments were performed in triplicate and data were presented as the mean ± standard deviation (n=3). Statistical analyses were carried out using SPSS software (SPSS Statistics v18, IBM, UK). Statistically significant differences among variables were performed using a One-way Analysis of Variance (ANOVA) followed by Student's

t-Test to establish any significant differences (*p<0.05).

Results and Discussion

Fabrication of ZP/OEO fibers and fibrous membranes

Two immiscible liquids were simultaneously infused into the coaxial device. For fiber generation, jetting stability is influenced by gravity, applied electrical force and media surface tension (Gao and others 2016b). Amongst all process parameters (e.g. applied voltage, media flow rate, collector distance and physical properties of solution), the applied voltage is a dominant factor in enabling ES and its optimization is essential for stable and continuous fiber generation (Cipitria and others 2011). When the electrical force between the capillary exit and ground electrode was increased to the optimal value, the liquid meniscus on the nozzle exit stretched into a conical shape, forming a cone-jet (mode). When the two solutions (OEO and ZP, flow rates 1.5 and 2.0 mL/h, respectively) were infused without any electrical force acting on the co-flow liquid system, the dripping mode was observed (**Figure 1b**). This comparatively simple liquid deformation and dripping behavior is attributed to gravitational, surface tension and mechanical syringe action. When the applied voltage was increased to ~19 kV, the co-flow liquid behavior at the nozzle exit transitioned from the dripping mode to the stable jetting mode, where typical characteristics of the Taylor cone were observed (**Figure 1c**). The auxiliary lines in the insets of **Figures 1b&c** demonstrate the immiscibility of OEO and ZP in the co-flow system, which is crucial for generating core-shell structures during the coaxial ES process.

In this study, the impact of varying enveloping ZP polymer concentration (25, 30 and 35 w/v%) on resulting composite (ZP/OEO) fibers was investigated. **Figures 2a-i** show surface morphology and size distribution of composite fibers prepared using ZP

solutions at various concentrations. Optical images (**Figures 2a, d&g**) suggest fiber production is achievable using all explored ZP solutions. Further inspection using SEM (**Figures 2b, e&h**) demonstrates the 35 w/v% solution is optimal when compared to 25 and 30 w/v% ZP solutions, due to the smooth surface morphology, which facilitates the encapsulation of core medium during the electrohydrodynamic process (Gao and others 2016a). Electrospun composite fibers prepared using 35 w/v% ZP solution appear more uniform. Higher magnification micrographs (**Figures 2c, f&i**) show composite fibers prepared using 35 w/v% ZP solution display ribbon like (flattened) morphology with smooth surface topography. Intermittent particle (beaded) and spindled morphologies are apparent for fibers (also ribbon like) prepared using solutions with varying ZP concentrations (25 and 30 w/v%). In addition, crinkled surface topography is also evident on composite fibers prepared from lower ZP concentrations. Rapid volatilization of ethanol in perfused ZP solution (during and subsequently after jetting) and unexpanded β-folds within ZP molecular structure result in ribbon and crinkled structures (Neo and others 2012; Jiang and others 2012). The resulting fiber diameter from structures engineered using solutions with ZP concentrations of 25, 30 and 35 w/v%, are 1.05±0.36, 2.30±0.43 and 1.61±0.41 μm, respectively, as shown in insets of **Figures 2c, f&i**.

In general, the rheological behavior, especially solution viscosity, is critical for fiber production and morphology type. Both ZP polymer concentration and molecular weight (M_w) influence solution viscosity (Rieger and others 2016). Polymer chain entanglement concentration (C_e) predicts the spinnability of the polymer solution used in this study, and represents the minimum polymer concentration necessary to fabricate electrospun fibers with a beaded morphology (McKee and others 2004; Palangetic and others 2014). The viscosity of ZP solutions (increasing from 5 to 35 w/v% ZP) shows an increase

before and after chain entanglement. In the current study, C_e was determined to be 16.8 w/v% for ZP solutions (**Figure 2j**), which suggests concentrations below this (C_e) value will yield particles, and fabrication of defect free composite fibers *via* ES require solutions with greater ZP concentrations (e.g. 35 w/v%).

Effect of flow rate

In a coaxial ES set-up, the driving liquid in the co-flowing process possesses the greater electrical conductivity (Loscertales and others 2002). ZP solutions exhibit greater electrical conductivities and viscosities, compared to co-flowing OEO (**Table 1**). The viscosity of ZP solutions increased with increasing polymer concentration (i.e. resulting viscosities were 422.2±0.9, 745.4±1.5, and 1197.0±3.0 mPa•S for solutions comprising 25, 30, and 35 w/v% ZP, respectively). The electrical conductivity decreased as the solution ZP concentration was increased (i.e. the electrical conductivities were 625.6±0.2, 611.2±0.5, and 599.5±0.6 μS/m for ZP concentrations of 25, 30, and 35 w/v%, respectively). The effect of flow rate on mean fiber diameter was investigated by varying the enveloping liquid (shell material, ZP infusion rate from 1.5 to 3.0 mL/h (1.5, 2.0, 2.5, and 3.0 mL/h). **Figure 3a** highlights the connection between composite (ZP/OEO) fiber diameter distribution and increasing ZP solution infusion rate.

Mean fiber diameters were 0.7±0.1, 0.9±0.2, 1.0±0.2 and 1.2±0.2 μm at infusion rates of 1.5, 2.0, 2.5 and 3.0 mL/h, respectively. An increase in the enveloping medium flow rate resulted in coarser fibers due to greater quantities of solution (and therefore ZP polymer content) contributing towards the fibrous shell. In addition, as fibers were engineered under stable jetting, the mean fiber diameter appeared uniform with a standard derivation of only ~0.2 μm.

400 **Effect of applied voltage**

401 The driving liquid (ZP solution) in the coaxial ES process dictates the co-flow behavior,
402 and electrical stress arising from this medium is transferred to the enveloped OEO *via*
403 viscosity. The effect of voltage on mean fiber size was assessed, using an applied
404 voltage range based on the stable jetting mode window (18.0-19.5 kV) (Bhardwaj and
405 Kundu 2010), with all other parameters (ZP solution concentration, flow rate of inner
406 and outer liquids, and collector distance) constant. Fiber diameter distributions are
407 shown in **Figure 3b**. Increasing the applied voltage results in finer fibers (i.e. mean
408 fiber diameters were 1.3±0.2, 1.0±0.2, 0.9±0.2 and 0.8±0.2 μm for applied voltages of
409 18.0, 18.5, 19.0 and 19.5 kV, respectively). This is due to an enhanced stretching force
410 at increased voltages (Bhardwaj and Kundu 2010). The standard deviation for mean
411 fiber diameters were also narrow for applied voltages between 18.0 and 19.5 kV. In this
412 range, the voltage is attributed to engineering within the stable jetting mode. At low
413 applied voltages, superfluous liquid accumulates at the nozzle exit (due to a low
414 drawing and stretching force) which intermittently impedes the ES process, giving rise
415 to fibers with a broader size distribution. At higher applied voltages a multi-jet mode
416 results, which also leads to production of fibers with a broader size distribution (Gao
417 and others 2016b).

418

419

420 **Encapsulation of OEO in ZP fiber matrix**

421 The coaxial ES technique has been shown to be more efficient for bioactive
422 encapsulation when compared to dispersion and emulsification methods (Moomand and
423 Lim 2014; Yao and others 2016a). Although the selected engineering process is crucial
424 for composite material integration, material properties also impact bioactive LC and EE.

OEO is volatile and therefore it's LC and EE need to be investigated to determine the suitability of the coaxial ES technique. For this, solutions with various ZP concentrations (contributing towards the shell matrix material) were investigated. As shown in **Figure 4**, both LC and EE of OEO in fibrous ZP membranes using low ZP concentrations (25 and 30 w/v%) were lower than those obtained using 35 w/v% ZP solution. The OEO LC values were 10.19±0.45, 15.41±0.57 and 22.28±0.27% when using 25, 30 and 35 w/v% ZP solutions, respectively. However, the EE values of OEO were 27.53±1.23, 42.81±1.58 and 53.68±0.78% when using 25, 30 and 35 w/v% ZP solutions, respectively. LC indicates the quantity, by comparison of the total mass, of OEO in the composite system, while EE defines the entrapment efficiency of OEO within the fibrous structure (i.e. in the core and ZP matrix). Differences in LC and EE are mainly due to the morphological variations of electrospun fibers, increase in polymeric chains arising from greater ZP concentrations and unequal distribution of ZP polymer surrounding encapsulated OEO (Yao and others 2016a). Non-uniform fibers, as shown in **Figures 2a&d,** lead to incomplete and poor encapsulation of OEO within the fiber matrix (i.e. core and also the ZP matrix), which accelerates the volatilization of OEO. Uniform fiber distribution obtained using 35 w/v% ZP solution enables encapsulation of OEO with a ZP shell matrix and fibers possess similar morphologies with equal ZP distribution along the length and width of individual fibers.

Surface hydrophilicity

Water contact angle (WCA) measurements provide an indication of membrane interaction at a liquid interface which are crucial for bio-related applications, such as cell adhesion, spreading and availability in the ambient environment (Liao and others 2016). WCAs of composite nonwovens prepared using various ZP solution

concentrations are shown in **Figure 5a**. Mean WCAs on membranes prepared using 25, 30 and 35 w/v% ZP solutions are 31.36±2.44, 49.65±1.97 and 63.08±2.97°, respectively, which indicate all composite membranes are hydrophilic. As shown in **Figures 5b&c**, the mean WCA on pure electrospun ZP membrane and OEO (medium scribed on an object slide) are 85.18±2.62 and 22.09±0.24°, respectively. This demonstrates pure ZP membranes are less hydrophilic than their composite systems. The difference between composite and pure ZP membrane hydrophilicity is due to ZP quantities within various samples. Greater ZP concentrations hinder diffusive movement of OEO from the inner core layer to the external region of fibers and thus membrane surface. Reduced LC and EE of OEO are observed for membranes prepared using lower ZP concentrations during coaxial ES; indicating incomplete OEO encapsulation. This is due to the easier vapor penetration through reduced polymer content (i.e. ZP loading volume is indicative of how much polymer will remain after evaporation). In addition, size distribution and surface morphology of electrospun fibers also influence the hydrophilicity (Yao and others 2016b). At low ZP concentrations, the non-uniform distribution of fibers and varied surface features (crinkled and beaded) lead to rougher surfaces as shown in **Figures 2c&f**. Besides, reduced fiber diameters limit the quantity of trapped air at the fiber membrane-water interface, which results in reduced WCAs (Liu and others 2016; Xu and others 2012).

Retention of OEO in fibrous membranes

The retention of free OEO and encapsulated OEO in ZP composite fibers was determined by measuring mass loss over 24 h. As shown in **Figure 6a,** the quantity of retained OEO decreased during the test period in all test groups. The retention of free OEO after 24h was only 2.76%, which indicates the volatile nature of OEO. The

greatest retention of OEO was 61.54% and was demonstrated by composite membranes prepared using 35 w/v% ZP solution. OEO retention from composite membranes prepared using 30 and 25 w/v% ZP solutions, was 41.12% and 39.44%, respectively. This trend in OEO retention is attributed to ZP content in the co-flow system. Larger quantities of ZP in the enveloping medium impede OEO evaporation from the composite system once atomized and exposed to air. **Figure 6a** shows OEO retention decreased sharply in the first hour (at ambient temperature, 25°C). After this point, OEO retention decreased gradually up to 8 hours after which it remained constant. **Figure 6b** shows OEO retention in the first hour. The retention of OEO was 47.46, 60.78 and 72.11% from composite membranes prepared from 25, 30 and 35 w/v% ZP solutions. The retention of free OEO was 7.14%. The sharp decline for free OEO is due to the rapid unhindered volatilization of OEO in air. As shown in **Figure 4**, low LC and EE of OEO in membranes prepared using 25 and 30 w/v% ZP solutions suggest greater OEO exposure to air. These results confirm membranes prepared from solution with higher ZP concentrations retain greater quantities of OEO within the fibrous composite system.

Infrared spectra

FTIR was used to investigate the effect of the coaxial ES process on chemical structure stability and material integration. Electrospun membranes were collected, dried for 24h and then analyzed. As shown in **Figure 7a**, infrared spectra of pure ZP powder, OEO and electrospun composite (ZP/OEO) fibers prepared with varying ZP solution concentrations were observed. The peaks at 1515 cm^{-1} and ~1650 cm^{-1} represent amide Ⅱ and amide Ⅰ bands in pure ZP powder, respectively (Gillgren and others 2009; Forato and others 2004). For the pure/free OEO, characteristic peak at 887 cm^{-1} represent non-polymethoxylated flavone residues in the oil, and the peaks at 957, 1050

500 and 1155 cm^{-1} indicate C-H stretching vibration of sinensetin, the C-H stretching
501 vibration of heptamethoxyflavone, and the C-O-C stretching vibration of tangeretin,
502 respectively, which are the polymethoxylated flavone constituents in OEO (Manthey
503 2006). Characteristic peaks are present in all spectra (**Figure 7a**) of ZP membranes
504 (prepared using 25, 30 and 35 w/v% ZP solutions) indicating successful encapsulation
505 and retention (post 24 hours drying) of OEO. The ZP amide Ⅰ band shifts to a lower
506 wavenumber as the ZP solution concentration is increased. As shown in **Figure 7b**, the
507 characteristic amide Ⅰ band is displayed at 1653, 1647 and 1646 cm^{-1} for membranes
508 prepared using 25, 30, and 35 w/v% ZP solutions, respectively. The shift in peak value
509 is due to the variation in the α-helix length; an increase in helical length leads to a lower
510 peak wavenumber. This arises from enhanced hydrogen bonding involving the C=O
511 group as the ZP solution concentration is increased (Dousseau and Pezolet 1990;
512 Torres-Giner and others 2008). Furthermore, longer α-helix structures also favor beaded
513 morphologies, which correlates with spindle and beaded morphologies obtained using
514 low ZP solution concentrations as previously shown in **Figure 2** (Moomand and Lim
515 2015b).
516
517 **Biological evaluation of electrospun fibrous membranes**
518 Cell viability reflects the potential toxic risks of different samples *in vitro*, expressed as
519 a percentage of viable cells within the total cell population, and calculated by comparing
520 the test group (fiber samples) to the control (no samples) (Güney and others 2014).
521 CCK-8 assay was used to evaluate cytotoxicity of electrospun fibrous discs. As shown
522 in **Figure 8a**, cell proliferations on both pure ZP and composite discs exhibit no
523 significant difference compared to the control group at 4 and 8 hours incubation time.
524 Cell viability remained at 105 and 100% for pure ZP and composite (ZP/OEO) discs,

525 respectively, at 4 hours incubation. After 8 hours, cell viability was 94 and 95% for pure
526 ZP and composite discs, respectively. These results clearly demonstrate negligible
527 cytotoxicity towards the HEK293T cell line, further supporting ZP utility as a
528 biomedical biopolymer (Jiang and others 2010).
529 Cell growth behavior was observed using an optical microscope. Cells were incubated
530 in medium with fibrous pure ZP and composite discs. As shown in **Figure 8b**, most
531 HEK293T cells exhibited growth and adherence. Cell morphology further confirmed
532 biocompatibility of ZP and composite discs at the selected assessment times. Cell
533 viability results indicate no significant variation among the test and control groups,
534 which demonstrates negligible cytotoxicity as shown in previous reports (Liao and
535 others 2016; Unlu and others 2010). The results suggest the non-toxicity of the
536 fabricated membranes and the potential to be used in food industry.
537
538 **Antimicrobial activity of ZP/OEO fibrous membranes**
539 The antimicrobial activity of composite fibrous discs was investigated using *E. coli* as
540 the test microorganism over a 24h incubation period. Membranes, and subsequently
541 discs with diameters of 15mm, prepared using 35 w/v% ZP solutions, were selected for
542 assessment, and pure ZP membrane was set as the control group (without OEO). Both
543 membranes were prepared using the same optimal ES conditions (applied voltage = 19
544 kV, flow rate of ZP solution = 2.0 mL/h, for composite membrane-flow rate of OEO =
545 1.5 mL/h, and collector distance = 12.0 cm). **Figures 9a, b&c**, show both disc samples
546 exhibit inhibition zones at 16, 20 and 24 h incubation. Moreover, inhibition zones
547 (diameter) of composite discs was significantly wider than pure ZP samples (i.e.
548 Inhibition zone=14.44±0.98 mm for composite discs, and 3.57±0.36 mm for pure ZP
549 discs at 16 h) as shown in **Figure 9d**. Fibrous mats present clear inhibition zones.

According to a previous study (Wen and others 2016b), the present results indicate fibrous mats to possess antimicrobial function.

Over the 24 h test period, the inhibition zone of each sample decreased slightly but showed no significant difference. Composite discs are non-toxic, biocompatible (Liao and others 2016) and demonstrate antimicrobial properties; elucidating potential applications in food packaging to address current challenges in food preservation.

Conclusion

In summary, optimized fibrous composite (ZP/OEO) membranes with mean diameters ranging from 750 to 1400 nm were fabricated using the coaxial ES technique. Composite fiber surface morphology and size distribution was regulated using ZP solution concentration, applied voltage and formulation flow rate. FTIR analysis indicates the successful and stable encapsulation of OEO within ZP fiber matrix. Variation in ZP solution concentration leads to the transformation of ZP chemical structure and further influences fiber morphology. By increasing the ZP concentration, fiber uniformity and continuity was achieved. In addition, LC, EE and retention of OEO were also enhanced. Greater ZP solution concentrations yield fibrous membranes (*via* coaxial-ES) with relatively superior hydrophobic properties. CCK-8 assay conducted on HEK293T cell lines demonstrated good cytocompatibility on both electrospun pure ZP and composite discs *in-vitro*. Cell morphology indicates no adverse effects on cell growth. Fibrous composite discs demonstrated antimicrobial activity using *E. coli*, indicating potential application as food packaging material for bioactive food preservation, such as prolonging fruit shelf-life and therefore sustainability.

Acknowledgements

This work was financially supported by the National Nature Science Foundation of China (No.81301304), the Fundamental Research Funds for the Central Universities, and the Key Technologies R&D Program of Zhejiang Province (2015C02035).

Author Contributions

Zhi-Cheng Yao performed the experimental work and analyzed the data. Si-Cong Chen contributed in the experiments of biological evaluation and antimicrobial activity test. Zeeshan Ahmad, Jie Huang, and Jing-song Li contributed towards data analysis, interpretation and discussion. Ming-Wei Chang directed and designed the experiments. All authors revised the manuscript and approved the final version.

References

Aceituno-Medina M, Mendoza S, Rodríguez BA, Lagaron JM, López-Rubio A. 2015. Improved antioxidant capacity of quercetin and ferulic acid during in-vitro digestion through encapsulation within food-grade electrospun fibers. Journal of Functional Foods 12:332-41.

Agarwal S, Wendorff JH, Greiner A. 2008. Use of electrospinning technique for biomedical applications. Polymer 49(26):5603-21.

Alvarenga Botrel D, Vilela Borges S, Victória de Barros Fernandes R, Dantas Viana A, Maria Gomes da Costa J, Reginaldo Marques G. 2012. Evaluation of spray drying conditions on properties of microencapsulated oregano essential oil. International Journal of Food Science & Technology 47(11):2289-96.

Appendini P, Hotchkiss JH. 2002. Review of antimicrobial food packaging. Innovative Food Science & Emerging Technologies 3(2):113-26.

Bhardwaj N, Kundu SC. 2010. Electrospinning: a fascinating fiber fabrication technique. Biotechnology advances 28(3):325-47.

Butz P, Fernandez GA, Lindauer GR, Dieterich S, Bognar A, Tauscher B. 2003. Influence of ultra high pressure processing on fruit and vegetable products. Journal of Food Engineering 56(2):233-6.

Chalco-Sandoval W, Fabra MJ, López-Rubio A, Lagaron JM. 2016. Development of an encapsulated phase change material via emulsion and coaxial electrospinning. Journal of Applied Polymer Science 133(36).

Chung D, Papadakis SE, Yam KL. 2003. Evaluation of a polymer coating containing triclosan as the antimicrobial layer for packaging materials. International journal of food science & technology 38(2):165-9.

Cipitria A, Skelton A, Dargaville T, Dalton P, Hutmacher D. 2011. Design, fabrication and characterization of PCL electrospun scaffolds—a review. Journal of Materials Chemistry 21(26):9419-53.

Dousseau F, Pezolet M. 1990. Determination of the secondary structure content of proteins in aqueous solutions from their amide I and amide II infrared bands. Comparison between classical and partial least-squares methods. Biochemistry 29(37):8771-9.

Eleftheriadou M, Pyrgiotakis G, Demokritou P. 2016. Nanotechnology to the rescue: using nano-enabled approaches in microbiological food safety and quality. Current Opinion in Biotechnology 44:87.

Fabra MJ, López-Rubio A, Lagaron JM. 2016. Use of the electrohydrodynamic process to develop active/bioactive bilayer films for food packaging applications. Food Hydrocolloids 55:11-8.

Fernandez A. 2009. Novel route to stabilization of bioactive antioxidants by encapsulation in electrospun fibers of zein prolamine. Food Hydrocolloids 23(5):1427-32.

Fisher K, Rowe C, Phillips CA. 2007. The survival of three strains of Arcobacter butzleri in the presence of lemon, orange and bergamot essential oils and their components in vitro and on food. Letters in applied microbiology 44(5):495-9.

Forato LA, Doriguetto AC, Fischer H, Mascarenhas YP, Craievich AF, Colnago LA. 2004. Conformation of the Z19 prolamin by FTIR, NMR, and SAXS. Journal of agricultural and food chemistry 52(8):2382-5.

Friedman M, Henika PR, Levin CE, Mandrell RE. 2010. Antimicrobial Wine Formulations Active Against the Foodborne Pathogens Escherichia coli O157: H7 and Salmonella enterica.

632 Journal of Food Science 71(71):M245-M51.
633 Güney G, Kutlu HM, Genç L. 2014. Preparation and characterization of ascorbic acid loaded solid
634 lipid nanoparticles and investigation of their apoptotic effects. Colloids and Surfaces B:
635 Biointerfaces 121:270-80.
636 Gao Y, Chang MW, Ahmad Z, Li JS. 2016a. Magnetic-responsive microparticles with customized
637 porosity for drug delivery. Rsc Advances 6(91).
638 Gao Y, Zhao D, Chang M-W, Ahmad Z, Li J-S. 2016b. Optimising the shell thickness-to-radius ratio
639 for the fabrication of oil-encapsulated polymeric microspheres. Chemical Engineering
640 Journal 284:963-71.
641 Gillgren T, Barker SA, Belton PS, Georget DM, Stading M. 2009. Plasticization of zein: a
642 thermomechanical, FTIR, and dielectric study. Biomacromolecules 10(5):1135-9.
643 Gram L, Ravn L, Rasch M, Bruhn JB, Christensen AB, Givskov M. 2002. Food
644 spoilage—interactions between food spoilage bacteria. International journal of food
645 microbiology 78(1):79-97.
646 Hongxu Qi, Hu P, Jun Xu A, Wang A. 2006. Encapsulation of Drug Reservoirs in Fibers by
647 Emulsion Electrospinning: Morphology Characterization and Preliminary Release
648 Assessment. Biomacromolecules 7(8):2327-30.
649 Jaworek A. 2008. Electrostatic micro- and nanoencapsulation and electroemulsification: a brief
650 review. Journal of Microencapsulation 25(7):443.
651 Jiang H, Wang L, Zhu K. 2014. Coaxial electrospinning for encapsulation and controlled release of
652 fragile water-soluble bioactive agents. Journal of Controlled Release 193:296.
653 Jiang H, Zhao P, Zhu K. 2007. Fabrication and characterization of zein-based nanofibrous scaffolds
654 by an electrospinning method. Macromolecular Bioscience 7(4):517.
655 Jiang Q, Reddy N, Yang Y. 2010. Cytocompatible cross-linking of electrospun zein fibers for the
656 development of water-stable tissue engineering scaffolds. Acta Biomaterialia 6(10):4042-51.
657 Jiang Y-N, Mo H-Y, Yu D-G. 2012. Electrospun drug-loaded core–sheath PVP/zein nanofibers for
658 biphasic drug release. International journal of pharmaceutics 438(1):232-9.
659 Li Y, Ai L, Yokoyama W, Shoemaker CF, Wei D, Ma J, Zhong F. 2013. Properties of
660 chitosan-microencapsulated orange oil prepared by spray-drying and its stability to
661 detergents. Journal of agricultural and food chemistry 61(13):3311-9.
662 Liakos I, Rizzello L, Scurr DJ, Pompa PP, Bayer IS, Athanassiou A. 2014. All-natural composite
663 wound dressing films of essential oils encapsulated in sodium alginate with antimicrobial
664 properties. International journal of pharmaceutics 463(2):137-45.
665 Liao N, Joshi MK, Tiwari AP, Park C-H, Kim CS. 2016. Fabrication, characterization and
666 biomedical application of two-nozzle electrospun polycaprolactone/zein-calcium lactate
667 composite nonwoven mat. Journal of the Mechanical Behavior of Biomedical Materials
668 60:312-23.
669 Liu K, Chen Q, Liu Y, Zhou X, Wang X. 2012. Isolation and Biological Activities of Decanal,
670 Linalool, Valencene, and Octanal from Sweet Orange Oil. Journal of Food Science
671 77(11):C1156–C61.
672 Liu Z, Zhao J-h, Liu P, He J-h. 2016. Tunable surface morphology of electrospun PMMA fiber using
673 binary solvent. Applied Surface Science 364:516-21.
674 Loscertales IG, Barrero A, Guerrero I, Cortijo R, Marquez M, Ganan-Calvo A. 2002. Micro/nano
675 encapsulation via electrified coaxial liquid jets. Science 295(5560):1695-8.

Maisanaba S, Pichardo S, Jordábeneyto M, Aucejo S, Cameán AM, Jos Á. 2014. Cytotoxicity and mutagenicity studies on migration extracts from nanocomposites with potential use in food packaging. 66(4):366-72.
Manthey JA. 2006. Fourier transform infrared spectroscopic analysis of the polymethoxylated flavone content of orange oil residues. Journal of agricultural and food chemistry 54(9):3215-8.
McCann JT, Li D, Xia Y. 2005. Electrospinning of nanofibers with core-sheath, hollow, or porous structures. Journal of Materials Chemistry 15(7):735-8.
McKee MG, Wilkes GL, Colby RH, Long TE. 2004. Correlations of solution rheology with electrospun fiber formation of linear and branched polyesters. Macromolecules 37(5):1760-7.
Moomand K, Lim L-T. 2014. Oxidative stability of encapsulated fish oil in electrospun zein fibres. Food Research International 62:523-32.
Moomand K, Lim L-T. 2015a. Effects of solvent and n-3 rich fish oil on physicochemical properties of electrospun zein fibres. Food Hydrocolloids 46:191-200.
Moomand K, Lim L-T. 2015b. Properties of encapsulated fish oil in electrospun zein fibres under simulated in vitro conditions. Food and Bioprocess Technology 8(2):431-44.
Neo YP, Ray S, Easteal AJ, Nikolaidis MG, Quek SY. 2012. Influence of solution and processing parameters towards the fabrication of electrospun zein fibers with sub-micron diameter. Journal of Food Engineering 109(4):645-51.
Neo YP, Ray S, Jin J, Gizdavic-Nikolaidis M, Nieuwoudt MK, Liu D, Quek SY. 2013. Encapsulation of food grade antioxidant in natural biopolymer by electrospinning technique: A physicochemical study based on zein–gallic acid system. Food chemistry 136(2):1013-21.
O'Bryan CA, Crandall PG, Chalova VI, Ricke SC. 2008. Orange Essential Oils Antimicrobial Activities against Salmonella spp. Journal of Food Science 73(6):M264–M7.
Palangetic L, Reddy NK, Srinivasan S, Cohen RE, McKinley GH, Clasen C. 2014. Dispersity and spinnability: Why highly polydisperse polymer solutions are desirable for electrospinning. Polymer 55(19):4920-31.
Quirós J, Boltes K, Rosal R. 2016. Bioactive Applications for Electrospun Fibers. Polymer Reviews 56(4):631-67.
Rieger KA, Birch NP, Schiffman JD. 2016. Electrospinning chitosan/poly (ethylene oxide) solutions with essential oils: Correlating solution rheology to nanofiber formation. Carbohydrate Polymers 139:131-8.
Sugumar S, Singh S, Mukherjee A, Chandrasekaran N. 2016. Nanoemulsion of orange oil with non ionic surfactant produced emulsion using ultrasonication technique: evaluating against food spoilage yeast. Applied Nanoscience 6(1):113-20.
Suppakul P, Miltz J, Sonneveld K, Bigger SW. 2003. Active Packaging Technologies with an Emphasis on Antimicrobial Packaging and its Applications. Journal of Food Science 68(2):408–20.
Torres-Giner S, Gimenez E, Lagaron J. 2008. Characterization of the morphology and thermal properties of zein prolamine nanostructures obtained by electrospinning. Food Hydrocolloids 22(4):601-14.
Torresalvarez C, González AN, Rodríguez J, Castillo S, Leosrivas C, Báezgonzález JG. 2016. Chemical composition, antimicrobial, and antioxidant activities of orange essential oil and

its concentrated oils. 00:1-7.
Unlu M, Ergene E, Unlu GV, Zeytinoglu HS, Vural N. 2010. Composition, antimicrobial activity and in vitro cytotoxicity of essential oil from Cinnamomum zeylanicum Blume (Lauraceae). Food & Chemical Toxicology An International Journal Published for the British Industrial Biological Research Association 48(11):3274-80.
Verghese K, Lewis H, Lockrey S, Williams H. 2015. Packaging's Role in Minimizing Food Loss and Waste Across the Supply Chain. Packaging Technology & Science 28(7):603-20.
Wang B, Zheng H, Chang MW, Ahmad Z, Li JS. 2016. Hollow polycaprolactone composite fibers for controlled magnetic responsive antifungal drug release. Colloids & Surfaces B Biointerfaces 145:757-67.
Wen P, Zhu D-H, Wu H, Zong M-H, Jing Y-R, Han S-Y. 2016a. Encapsulation of cinnamon essential oil in electrospun nanofibrous film for active food packaging. Food Control 59:366-76.
Wen P, Zhu DH, Feng K, Liu FJ, Lou WY, Li N, Zong MH, Wu H. 2016b. Fabrication of electrospun polylactic acid nanofilm incorporating cinnamon essential oil/β-cyclodextrin inclusion complex for antimicrobial packaging. Food Chemistry 196:996-1004.
Xu X, Jiang L, Zhou Z, Wu X, Wang Y. 2012. Preparation and properties of electrospun soy protein isolate/polyethylene oxide nanofiber membranes. Acs Appl Mater Interfaces 4(8):4331.
Yang J-M, Zha L-s, Yu D-G, Liu J. 2013. Coaxial electrospinning with acetic acid for preparing ferulic acid/zein composite fibers with improved drug release profiles. Colloids and Surfaces B: Biointerfaces 102:737-43.
Yao Z-C, Chang M-W, Ahmad Z, Li J-S. 2016a. Encapsulation of rose hip seed oil into fibrous zein films for ambient and on demand food preservation via coaxial electrospinning. Journal of Food Engineering 191:115-23.
Yao Z-C, Gao Y, Chang M-W, Ahmad Z, Li J-S. 2016b. Regulating poly-caprolactone fiber characteristics in-situ during one-step coaxial electrospinning via enveloping liquids. Materials Letters 183:202-6.
Ziani K, Fang Y, McClements DJ. 2012. Fabrication and stability of colloidal delivery systems for flavor oils: Effect of composition and storage conditions. Food Research International 46(1):209-16.

Tables

Table 1. Viscosity and electrical conductivity of solutions used in this study

	25 w/v% ZP	30 w/v% ZP	35 w/v% ZP	OEO
Viscosity (mPa•S)	422.2±0.9	745.4±1.5	1197.0±3.0	6.7±0.5
Elec. Conduct. (μS/m)	625.6±0.2	611.2±0.5	599.5±0.6	<0.1

Figures

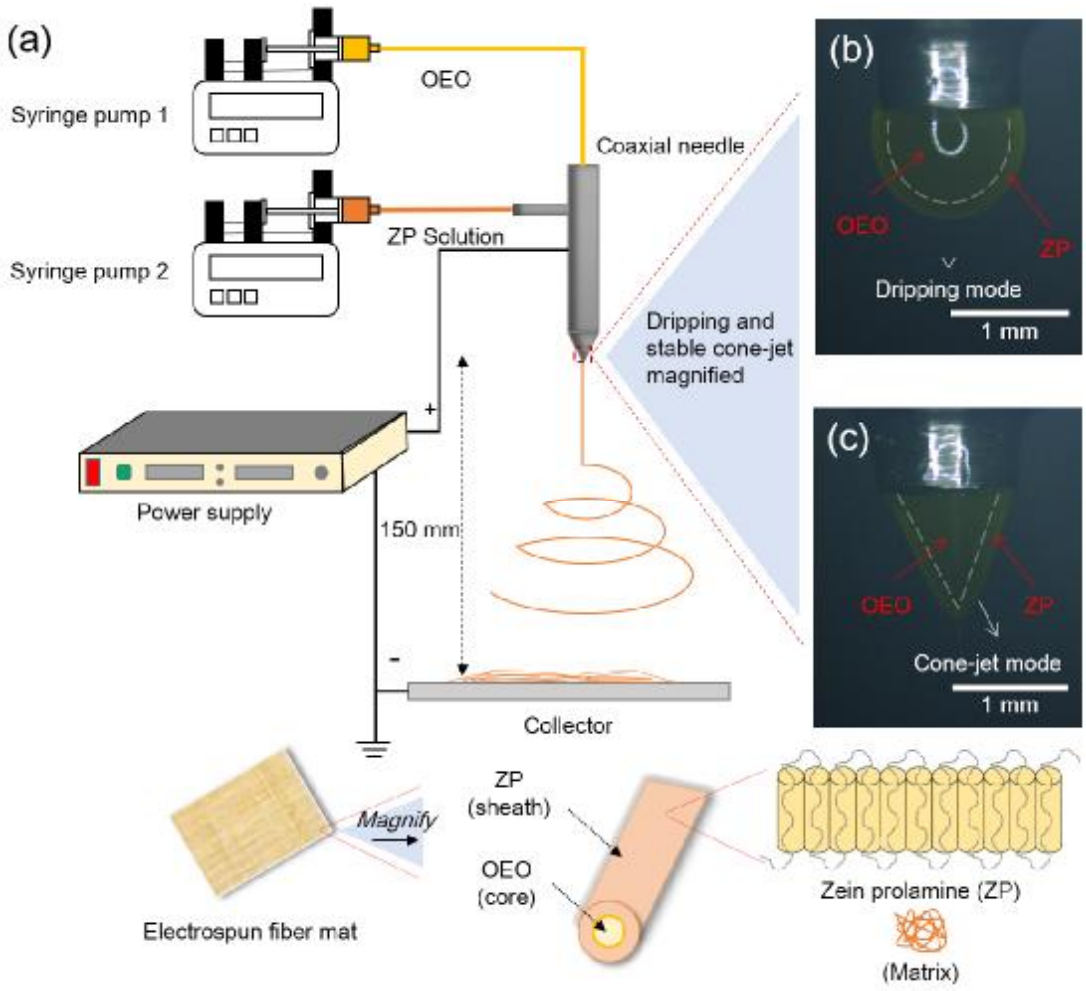

Fig. 1. (a) Schematic diagram of coaxial system used in this study. Inserts show two images exhibiting characteristic coaxial electrospinning modes; (b) dripping mode at 0 kV and (c) cone-jet mode at 19 kV. [For both images, flow rate of the enveloping medium (ZP) = 2.0 mL/h, flow rate of the enveloped medium (OEO) = 1.5 mL/h]

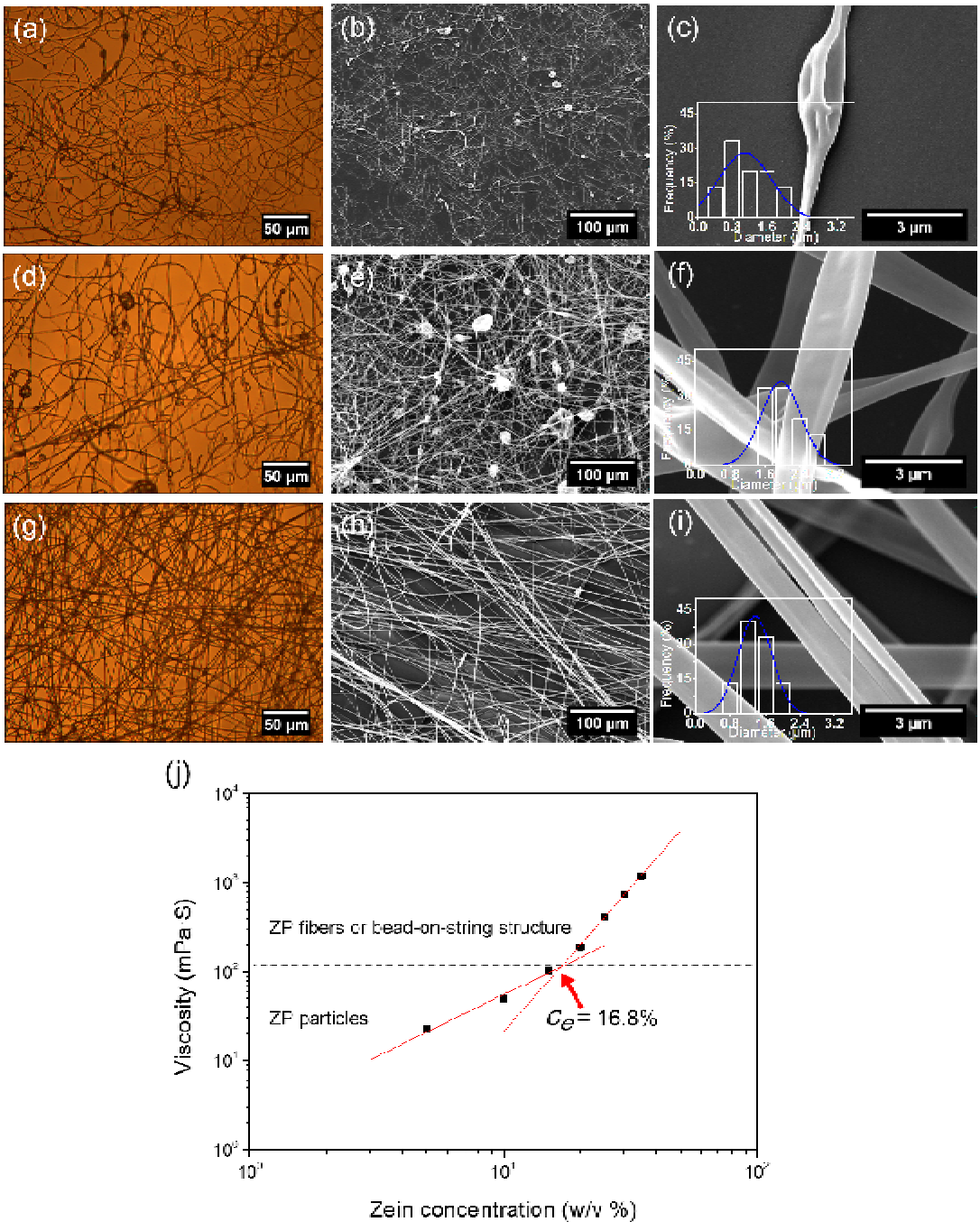

Fig. 2. Optical micrographs of electrospun fibers obtained at ZP solution concentrations of: (a) 25, (d) 30, and (g) 35 w/v%. Scanning electron micrographs of electrospun fibers obtained at ZP solution concentrations of: (b) 25, (e) 30, and (h) 35 w/v%. Micrographs (c), (f), and (i) are higher magnifications of (b), (e), and (h), respectively, with size distribution insets. (j) Fiber forming dynamics as a function of ZP solution viscosity *vs.* polymer (ZP) concentration.

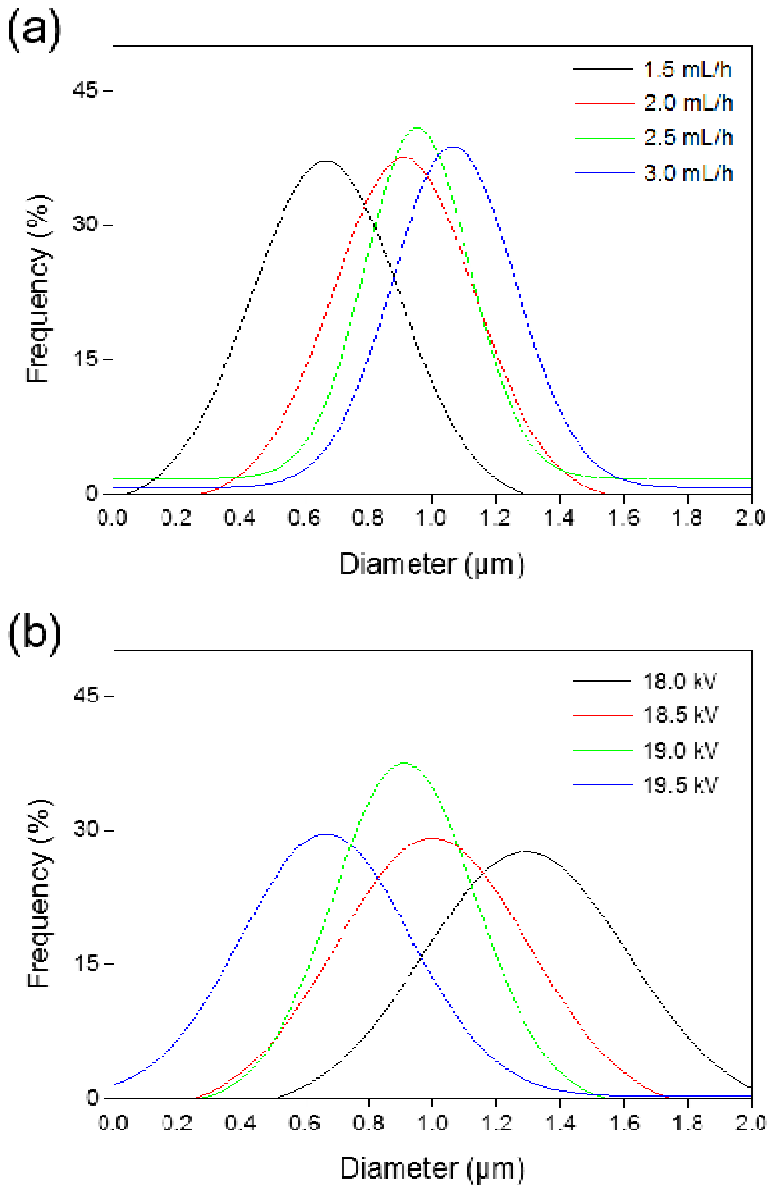

Fig. 3. Gaussian curves of fibers size distribution generated with different process parameters. (a) Effect of enveloping medium flow rate on mean fiber diameter. [experimental conditions: ZP solution concentration = 35 w/v%, enveloped medium flow rate (OEO) = 1.5 mL/h, applied voltage = 19.0 kV and collector distance = 12.0 cm]. (b) Effect of applied voltage on mean fiber diameter. [experimental conditions: ZP solution concentration = 35 w/v%, flow rate of the enveloping medium (ZP) = 2.0 mL/h, flow rate of the enveloped medium (OEO) = 1.5 mL/h, and collector distance = 12.0 cm].

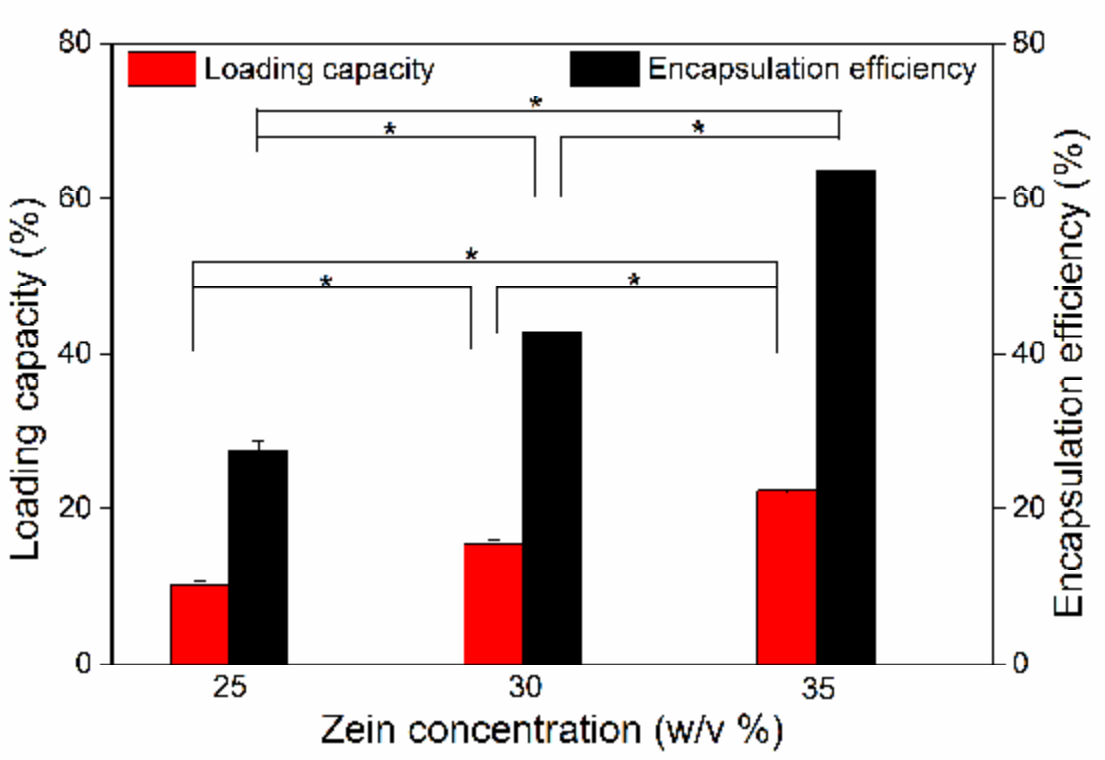

786

787 **Fig. 4.** Loading capacity and encapsulation efficiency of OEO using ZP solutions

788 (during ES) with various concentrations. (*P<0.05)

789

790

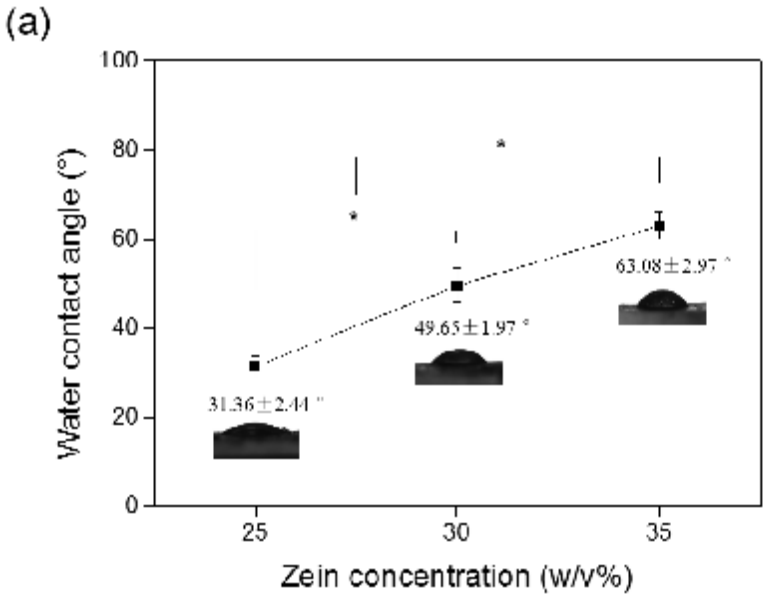

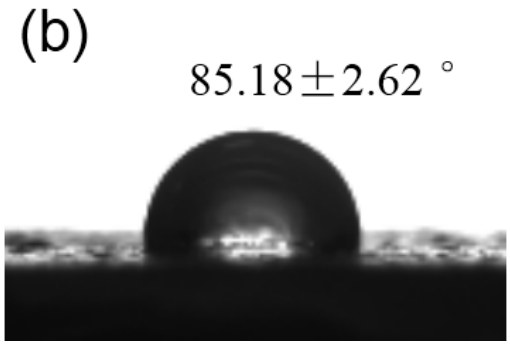

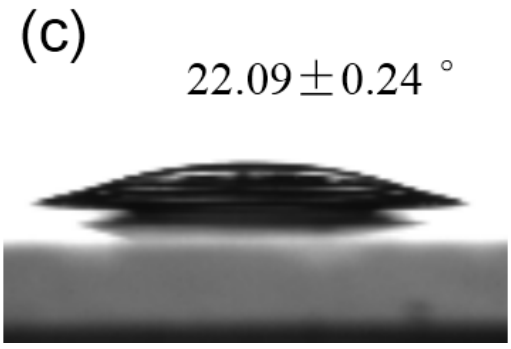

Fig. 5. Water contact angles (WCAs) on fibrous membrane samples and OEO. (a) WCAs on electrospun ZP/OEO coaxial fibrous membranes prepared using various ZP solution concentrations (*P<0.05), (b) WCA on single needle electrospun ZP membrane, (c) WCA on pure OEO.

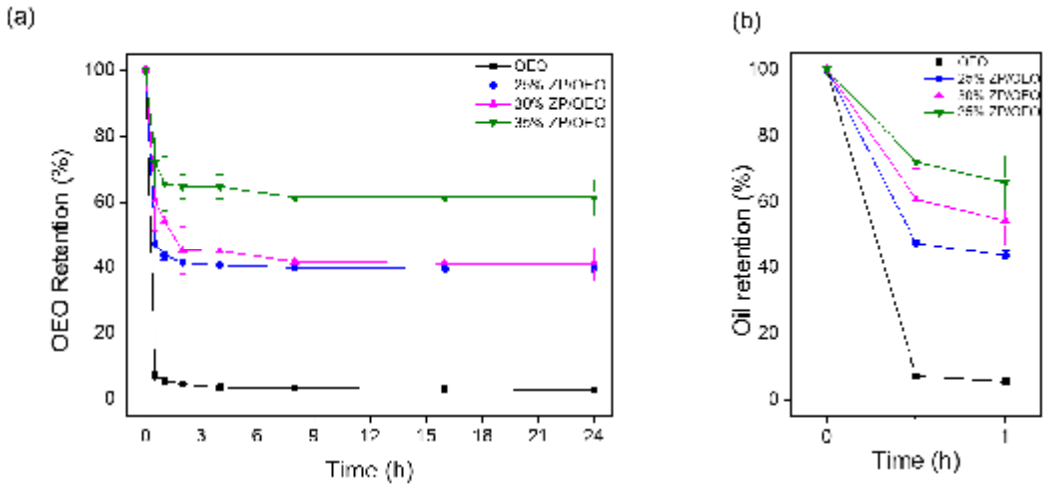

799

800 **Fig. 6.** Retention of free OEO and encapsulated OEO in fiber during (a) 24h, (b) 1h.

801

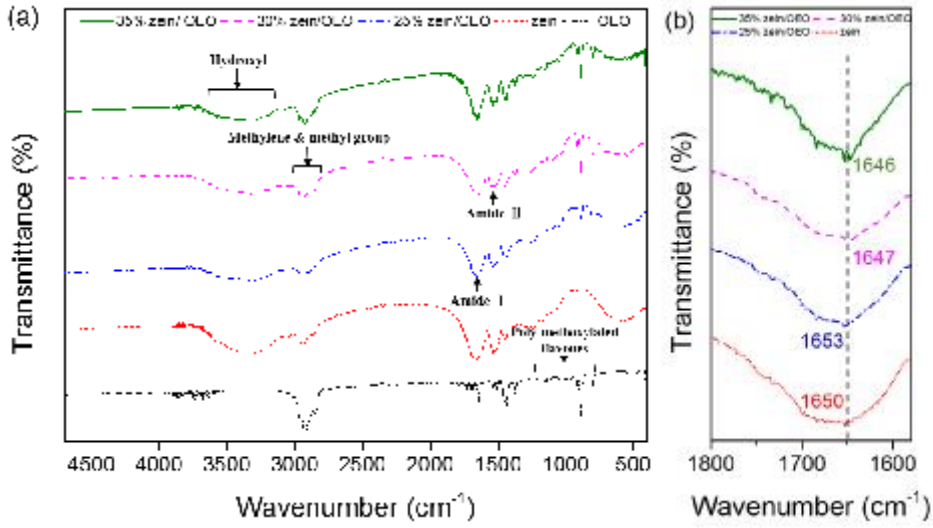

802

803 **Fig. 7.** FTIR spectra of materials and samples in this study. (a) FTIR spectra of pure ZP

804 electrospun membrane, pure OEO and ZP/OEO fibrous membranes fabricated with

805 different ZP solution concentrations. (b) The shift in characteristic amide Ⅰ band for ZP.

806

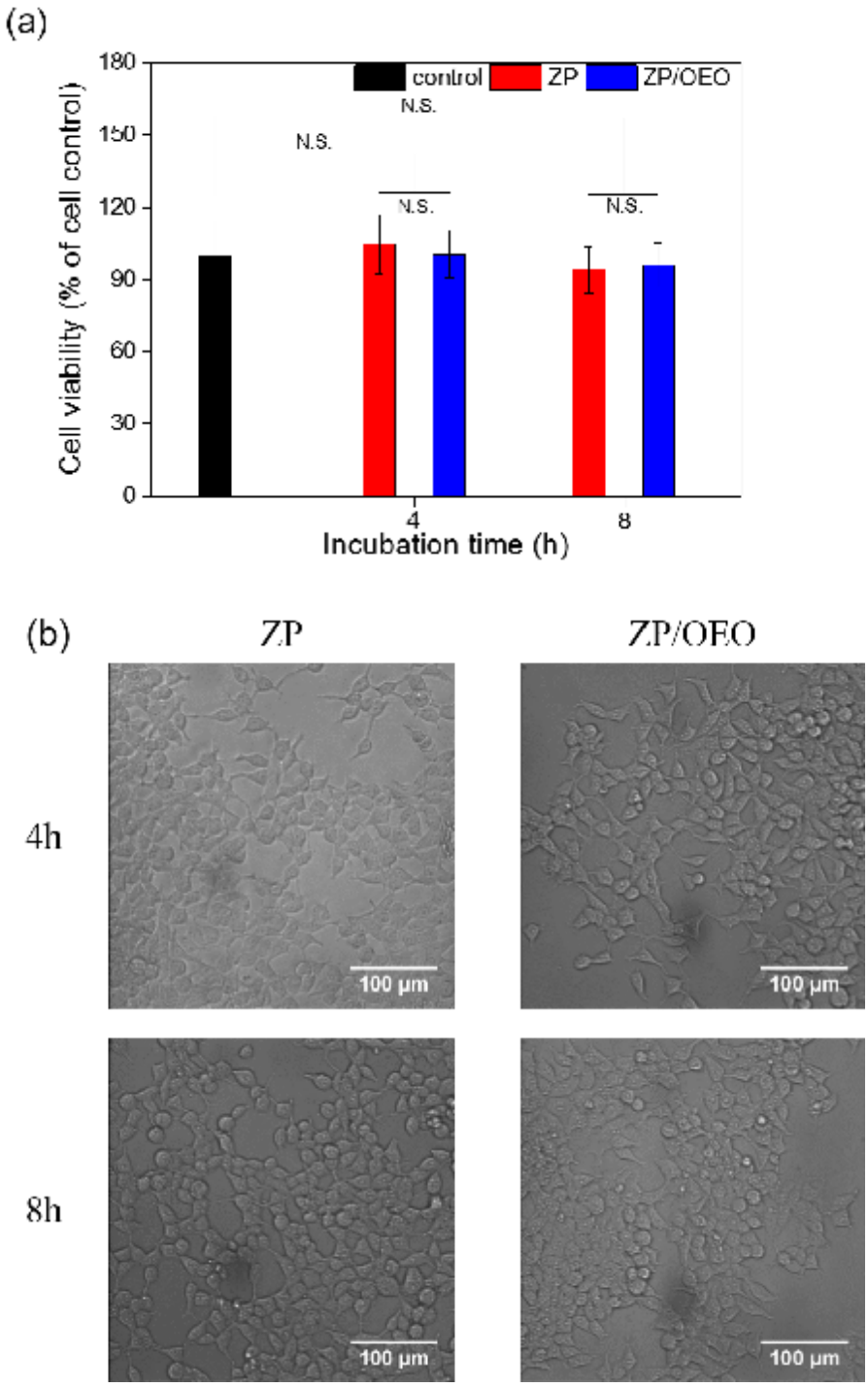

Fig. 8. Evaluating cell viability using CCK-8 assay. (a) CCK-8 test on electrospun ZP and ZP/OEO membranes after 4 and 8 hours cell culture. The viability of the control cells was set to 100%. (N.S. means no significant difference) (b) Optical micrographs showing cytocompatibility of ZP and ZP/OEO fibrous membranes incubated with HEK293T cells after 4 and 8 hours.

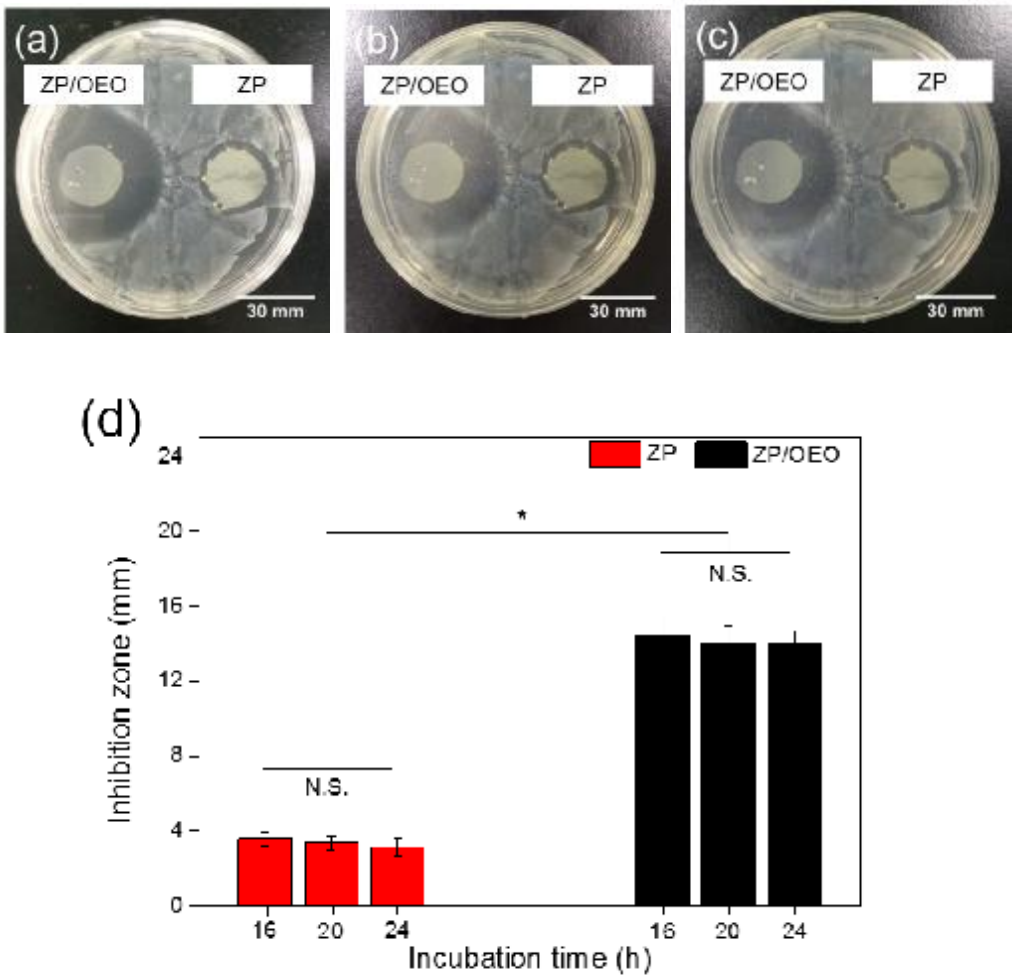

Fig. 9. Inhibition zones (E. coli) generated using ZP membranes and 35 w/v % ZP/OEO membranes at (a) 16 (b) 20 and (c) 24h. (d) Diameter of inhibition zones at various assessment times. (N.S. means no significant difference; *$p<0.05$, comparing inhibition zone areas of ZP and ZP/OEO groups at identical time intervals).